Analysis of Curved Bridges Crossing Fault Rupture Zones

R.K.Goel, B.Qu & O.Rodriguez
Dept. of Civil and Environmental Engineering, California Polytechnic State University, San Luis Obispo, CA 93407, USA

SUMMARY:
This paper evaluates the adequacy of two approximate analysis procedures, the fault rupture-response spectrum analysis (FR-RSA) procedure and the fault rupture-linear static analysis (FR-LSA) procedure, in estimating the seismic demands for curved bridges crossing fault rupture zones. The FR-RSA and FR-LSA procedures were originally developed for ordinary straight bridges crossing fault-rupture zones and have been proved valid in a prior investigation. In this investigation the two approximate procedures are revisited for evaluation of two Californian curved bridges (one with three spans and the other with four spans) crossing fault rupture zones. Seismic demands obtained from the approximate procedures are compared with those from the nonlinear response history analysis (RHA) which is more rigorous but may be too onerous for practical application. Results show that the FR-RSA and FR-LSA procedures which require less modelling and analysis efforts provide reasonable seismic demand estimates for curved bridges crossing fault zones.

Keywords: seismic demand, curved bridge, crossing fault rupture zones

1. INTRODUCTION

While avoiding construction of the bridges crossing fault ruptures might be the best approach, such situations are not always permissible in regions of high seismicity such as California. Currently, 5% of the Californian bridges cross fault ruptures or lie very close to fault-rupture zones. In a recent earthquake in Wenchuan, China, severe damages were observed from bridges crossing fault ruptures, demonstrating the vulnerability of such bridges (Kawashima et al. 2009). In response to the observed damages, extensive research efforts have been made to develop more effective and well-organized procedures to estimate the seismic demands for bridges crossing fault rupture zones.

Goel and Chopra (2008) developed two simplified procedures, namely, the Fault Rupture-Response Spectrum Analysis (FR-RSA) and Fault Rupture-Linear Static Analysis (FR-LSA) procedures to estimate the seismic demands for straight ordinary bridges crossing fault ruptures. These two procedures estimate the seismic demands by superposing the peak values of quasi-static and dynamic bridge responses. The peak quasi-static response in both methods is computed by nonlinear static analysis of the bridge under the ground displacement associated with fault rupture. In FR-RSA and FR-LSA, the peak dynamic responses are respectively estimated from the combination of the peak modal responses using the complete quadratic combination (CQC) and the linear static analysis of the bridge under appropriate equivalent seismic forces, respectively. The FR-RSA and FR-LSA procedures have been confirmed to be adequate for straight ordinary bridges through result comparisons against the nonlinear response history analysis (RHA) procedure, which is a more rigorous approach requiring excessive modelling and computational efforts. This paper revisits these approximate procedures and further evaluates their adequacy in the analysis of two curved bridges, which reflect the current bridge design and construction practice in California. The following briefly reviews the FR-RSA and FR-LSA procedures followed by description of the considered bridges and the corresponding finite element models together with result comparisons and discussions.

2. EXISTING APPROXIMATE ANLAYSIS PROCEDURES

The FR-RSA and FR-LSA procedures were developed by superposing the peak values from quasi-static (r_o^s) and dynamic (r_o) parts, to form a total system response r_o^t for straight ordinary bridges. The quasi-static and dynamic components are respectively found through: (1) static analysis of the nonlinear bridge model with all support displacements applied simultaneously; and (2) conducting either the response spectrum or static procedures on the linear bridge model under the fault-normal and fault-parallel ground motions.

Both methods utilize special features of the spatially varying ground motions in fault-rupture zones where displacements at support l can be approximated as:

$$u_{gl}(t) = \alpha_l u_g(t) \tag{2.1}$$

where $u_g(t)$ is the displacement history at a reference location, and α_l is the proportionality constant for the l^{th} support motion (Goel and Chopra 2008).

2.1. FR-RSA Procedure

As described above, the FR-RSA procedure combines the bridge response based on:

$$r_o^t = \left|r_o^s\right| + \left|r_o^{FN}\right| + \left|r_o^{FP}\right| \tag{2.2}$$

where r_o^{FN} and r_o^{FP} represent the peak bridge responses caused by the fault-normal and fault-parallel ground motions, respectively.

In the FR-RSA procedure, the periods and mode shapes of the bridge are obtained based on eigenvalue analysis of the linear bridge model; the effective influence vector for fault-parallel motion is determined based on the special ground motions described in Eqn. 2.1 while the effective influence vector for the fault-normal motions is the same as conventional response spectrum analysis. In this investigation, the response quantities associated with each mode are combined using the CQC rule.

2.2. FR-LSA Procedure

Similar to the FR-RSA procedure, the FR-LSA procedure also combines the estimates of bridge quasi-static response and dynamic response. However, different from the FR-RSA procedure, the dynamic response of the bridge is determined from a static analysis of the bridge under appropriate equivalent seismic forces. As a result, the combined bridge response can be calculated from Eqn. 2.3.

$$r_o^t = \max\left|r_o^s + r_o^{FN.i} + r_o^{FP.j}\right| \quad \left(i = 1 \text{ or } 2; j = 1 \text{ or } 2\right) \tag{2.3}$$

where $r_o^{FN.i}$ and $r_o^{FP.j}$ represent the peak bridge responses caused by the fault normal and fault parallel ground motions, respectively, which can be determined from the linear static analysis.

As recognized in Goel and Chopra (2008), dynamic response of the bridge may be conservatively estimated by assuming the spectral acceleration of the bridge equal to 2.5 times the peak ground acceleration and distributing the seismic force using a proper effective influence vector shown in Fig. 2.1, which is specifically determined for the ground motion described in Eqn. 2.1.

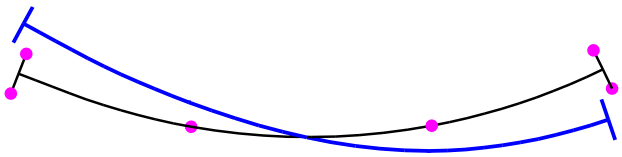

Figure 2.1. Sketch of the effective influence vector for a bridge crossing fault rupture zones

Given that peak dynamic response can be either positive or negative, four cases of equivalent static force distributions are considered in response calculations:

$$
\begin{aligned}
&r_o^{FN.1} \text{caused by } 2.5 m l_{eff\_FN} \mathrm{PGA}_{FN} \qquad r_o^{FN.2} \text{caused by } -2.5 m l_{eff\_FN} \mathrm{PGA}_{FN} \\
&r_o^{FP.1} \text{caused by } 2.5 m l_{eff\_FP} \mathrm{PGA}_{FP} \qquad r_o^{FP.2} \text{caused by } -2.5 m l_{eff\_FP} \mathrm{PGA}_{FP}
\end{aligned}
\tag{2.4}
$$

where m represents the mass matrix in the equation of motion; l_{eff_FN} and l_{eff_FP} respectively represent the effective influence vectors for fault-normal and fault-parallel motions; PGA_{FN} and PGA_{FP} respectively represent the peak ground accelerations of the fault normal and fault parallel motions.

3. MODELING OF THE SELECTED BRIDGES

To further verify the adequacy of the abovementioned approximate procedures, two curved bridges respectively designated as Bridges 55-0837S and 55-0939G in California were selected. Bridge 55-0837S is a three-span curved bridge built in 2000; 55-0939G is a four-span curved bridge built in 2001. Fig. 3.1 shows the selected bridges.

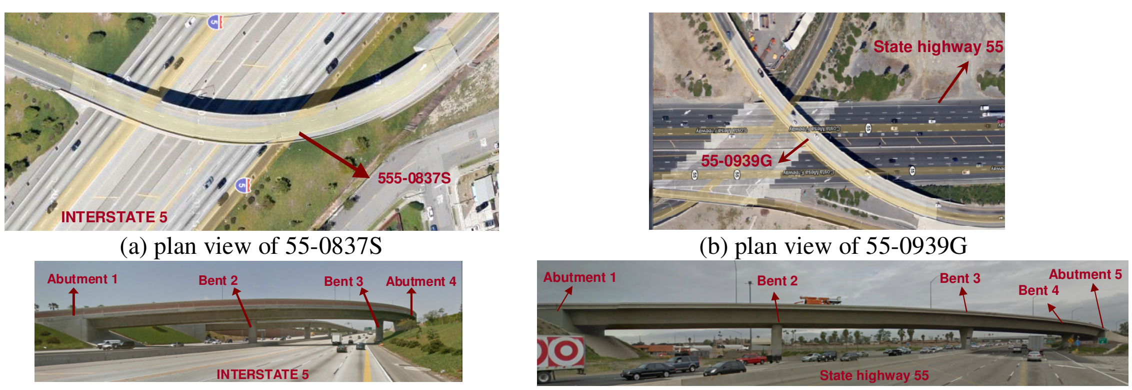

(a) plan view of 55-0837S (b) plan view of 55-0939G

(c) elevation of 55-0837S (d) elevation of 55-0939G

Figure 3.1. Selected Bridges

3.1. Finite Element Models

The original finite element models of the selected bridges were set up using the Open System for Earthquake Engineering Simulation (OpenSees) (Mazzoni et al. 2006), by the researchers from the University of California, Irvine (UCI) for other research purposes. The original finite element models were modified to be linear and nonlinear models in this investigation. In both linear and nonlinear models, the bridge decks were modelled using elastic beam-column elements (elasticBeamColumn in OpenSees). The bents in the linear models were modelled using elastic beam-column elements; however, the bents in the nonlinear models were considered using the beam-column elements with distributed plasticity and linear curvature distribution (dispBeamColumn in OpenSees). To consider the soil-structure interaction, spring elements were assigned at the bent bases. Properties of the springs were determined according to the California Department of Transportation (Caltrans) Seismic Design Criteria (SDC) (Caltrans 2010).

Soil springs were also assigned at the bridge abutment locations to take into account the abutment restraining effects. Along the transverse direction, linear elastic springs with stiffness equal to 50% of the elastic transverse stiffness of the adjacent bent were defined as recommended in the Caltrans SDC (Caltrans 2010). In the longitudinal direction, the elastic-perfectly plastic gap springs specified in the original nonlinear models were converted to an elastic compression only springs using the Caltrans SDC recommendations (see Fig. 3.2) where stiffness of the longitudinal spring, K_{eff}, can be determined from:

$$K_{eff} = \frac{P_{bw}}{\Delta_{eff}} = \frac{P_{bw}}{\Delta_{gap} + P_{bw}/K_{abut}} \tag{3.1}$$

where P_{bw} is the passive pressure force resisting movement at the abutment, and Δ_{gap} is determined from the elastic-perfectly plastic gap springs.

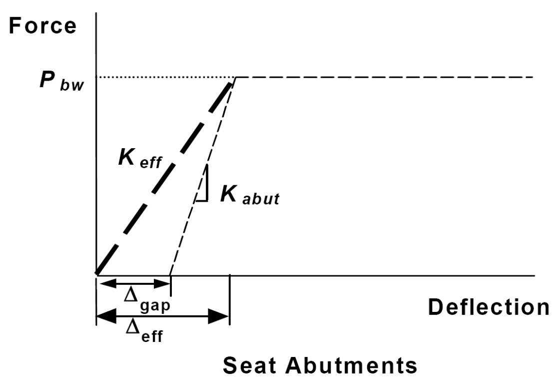

Figure 3.2. Simplification of longitudinal abutment springs
(Adapted from Caltrans 2010)

Conceptually, the displacement restraining effect along the longitudinal direction due to the presence of abutments depends on the magnitude of the longitudinal displacement of the bridge. A larger longitudinal bridge displacement indicates more severe damages occurring at the abutments. As a result, a smaller stiffness should be assigned to the abutment longitudinal springs to consider the less significant restraining action. Accordingly, the Caltrans SDC suggest a stiffness varying between 0.1 to 1.0 K_{eff} for the longitudinal abutment springs, which can be further determined from an iterative process based on the longitudinal displacement of the bridge. To validate the approximate procedures under a broader range of the parameters, three stiffness values -- $0.10K_{eff}$, $0.55K_{eff}$, and $1.00K_{eff}$ -- were considered in the investigation.

3.2. Selected Ground Motions

Ground motion pairs were selected to match the design spectrum provided by Caltrans SDC (Caltrans, 2010). Due to the limited number of actual ground motions recorded very close to actual ruptured faults (less than 100m), ground motion simulations are the only method to obtain time histories for this analysis. These simulated time histories were required to incorporate the near-fault source radiation pattern and to account for far- and near-field seismic radiation during rupture process as well as the sudden elastic rebound. A set of 10 ground motion pairs were provided by Caltrans for the investigation (Shantz and Chiou, 2011). Fig. 3.3 compares the geometric means of the response spectra of the ground motions and the idealized Caltrans SDC design spectrum.

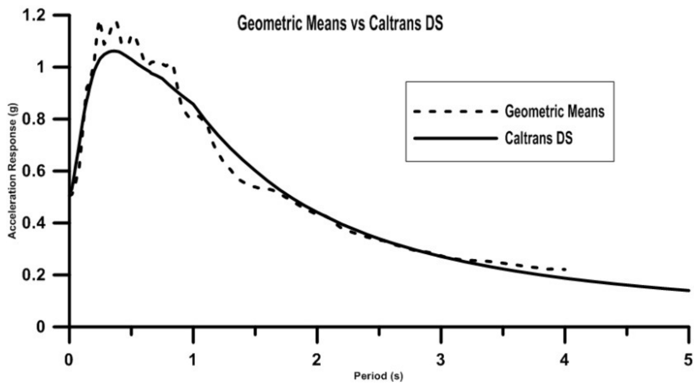

Figure 3.3. Caltrans design spectrum and elastic response spectra of the considered ground motions

3.3. Fault Locations and Bridge Orientations

For Bridge 55-0837S, the fault rupture line is assumed to be between Bents 2 and 3; for Bridge 55-0939G, two cases of fault locations were considered, i.e., assuming the fault rupture lines respectively between Bents 2 and 3 and between Bents 3 and 4 as shown in Fig. 3.4.

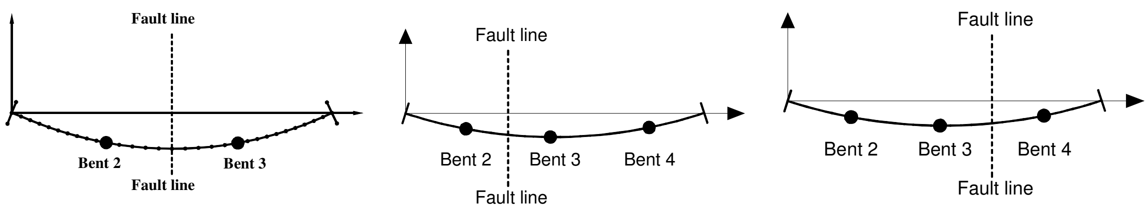

(a) Bridge 55-0837S (fault between Bents 2 and 3)

(b) Bridge 55-0939G (fault between Bents 2 and 3)

(c) Bridge 55-0939G (fault between Bents 3 and 4)

Figure 3.4. Illustration of fault locations

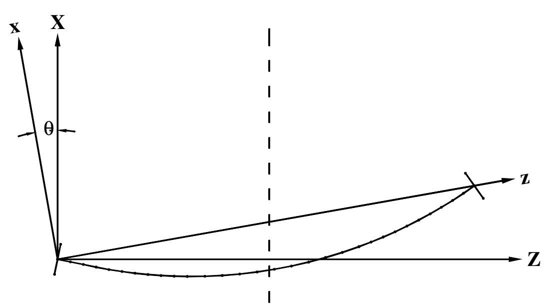

Figure 3.5. Definition of bridge orientation angle

Another parameter considered in the investigation is the fault-line-to-bridge orientation angles. In an actual case, the fault rupture may not always orient perpendicular to the line connecting the two abutments of the bridge. It is necessary to evaluate the adequacy of the approximate procedures under a broader ranges of the angles from the fault rupture to the line connecting the two abutments of the bridge. To this end, the orientation angle illustrated in Fig. 3.5 is introduced and Table 3.1 lists the selected angles considered in the investigation. It is noted that maximum and minimum angles represent the extreme cases of bridge orientations for which the fault will remain between the two adjacent bents.

Table 3.1. Selected Bridge Orientations

Bridges	Selected Orientation Angles
55-0837S	-51°, -36°, -21°, -6°, 0°, and 9°
55-0939G (fault line between Bents 2 and 3)	-36°, -15°, 0°, 18°, 41°, and 55°
55-0939G (fault line between Bents 3 and 4)	-34°, -15°, 0°, 18°, and 41°

4. RESULT DISCUSSIONS AND CONCLUSIONS

As described above, three parameters were varied in the investigation: the stiffness of the longitudinal abutment springs (selected to be $0.10K_{eff}$, $0.55K_{eff}$, and $1.00K_{eff}$), the bridge orientation angles (selected to be the values listed in Table 3.1), and the different fault locations (see Fig. 3.4), to evaluate the robustness and adequacy of the FR-RSA and FR-LSA procedures under the practical ranges of the parameters. Due to the space constraint, only results from a few selected cases are presented in Figs. 4.1 to 4.3. Results for other considered cases are available elsewhere (Rodriguez 2012).

The bridge demands compared in Figs. 4.1 to 4.3 include the peak values of the longitudinal and transverse abutment displacements and the peak values of the resultant bent displacements. In addition, the results from the FR-RSA and FR-LSA procedures are differentiated into two categories: GM and SD, as shown in the figures, which respectively represent the results obtained using the spectral accelerations from the response spectra of ground motion pairs and the idealized Caltrans SDC design spectrum. Moreover, for the results from the GM category, the average values of the bridge responses from the 10 ground motions pairs are presented. As compared in the figures, the results consistently show that the FR-RSA procedure provides reasonable estimates for the seismic demands of the bridge, and the FR-LSA procedure is conservative in some cases due to the use of a conservative estimate of response spectral acceleration when compared with results from the nonlinear RHA procedure. Based on the results from this investigation, it is found the FR-RSA and FR-LSA procedures can be extended in seismic analysis and design of curved bridges crossing fault zones.

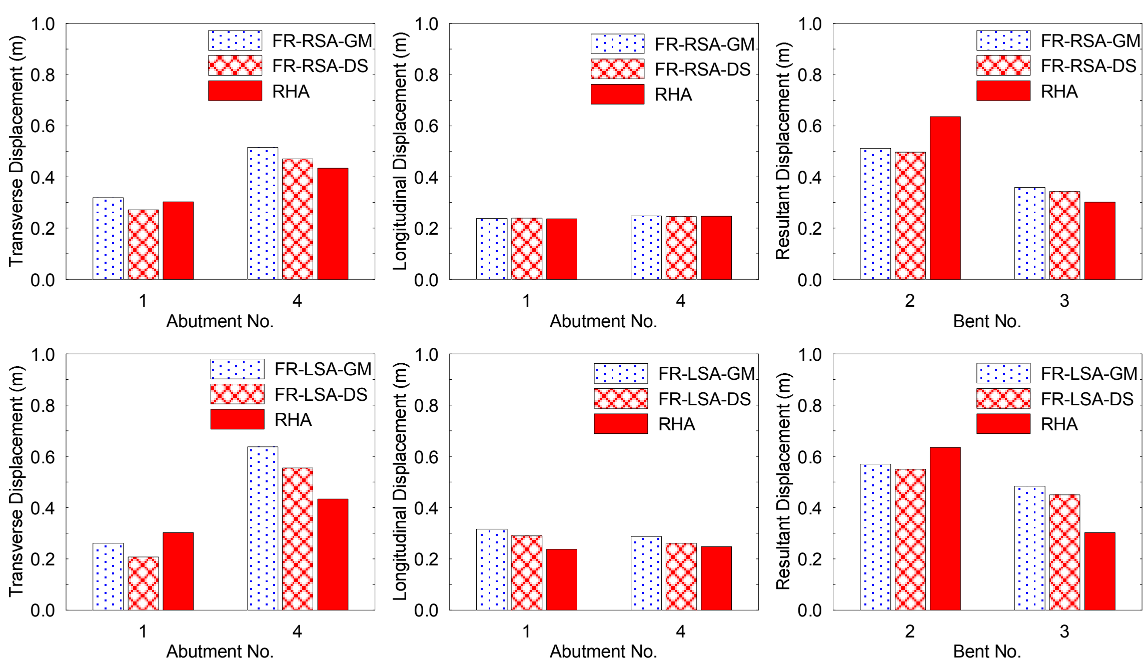

Figure 4.1. Result Comparisons of Bridge 55-0837S ($\theta = 0°$; longitudinal abutment stiffness= 0.1 K_{eff})

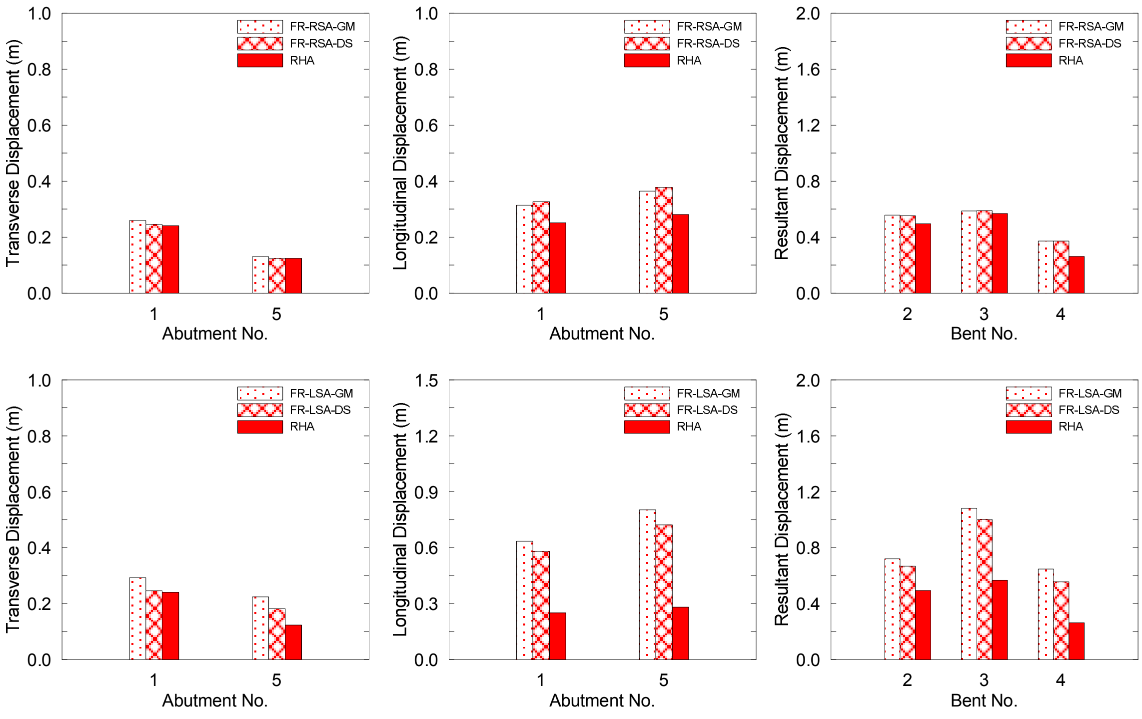

Figure 4.2. Result Comparisons of Bridge 55-0939G
($\theta = 0°$; longitudinal abutment stiffness= 0.1 K_{eff}, fault line between Bents 2 and 3)

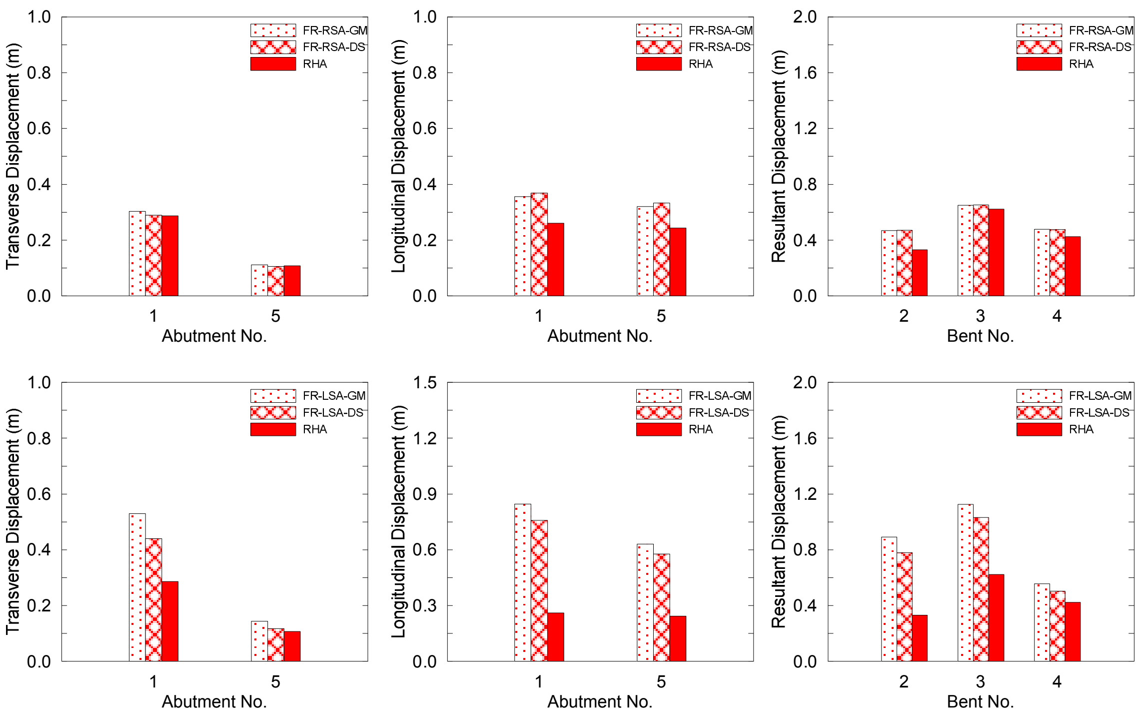

Figure 4.3. Result Comparisons of Bridge 55-0939G
($\theta = 0°$; longitudinal abutment stiffness= 0.1 K_{eff}, fault line between Bents 3 and 4)

AKCNOWLEDGEMENT
The research reported in this paper is supported by Caltrans under Contract No. 65A0379 with Dr. Allaoua Kartoum as the project manager. The support is gratefully acknowledged. We acknowledge Drs. Tom Shantz and Brian Chiou from the Division of Research and Innovation of Caltrans who simulated the ground motions used in this investigation. We are also grateful to Mark Yashinsky, Foued Zayati, Mark Mahan, and Toorak Zokaie of Caltrans for their useful feedback on this research investigation. Moreover, the original finite element bridge model was developed by Dr. Farzin Zareian from UCI.

REFERENCES

Caltrans. (2010). Seismic Design Criteria (Version 1.6 ed.) California Department of Transportation, Sacramento, CA (http://ww.dot.ca.gov)

Goel, R. K., and Chopra, A. K. (2008). Analysis of Ordinary Bridges Crossing Fault-Rupture Zones. **Rep. No. UCB-EERC-2008/01**, *Earthquake Engineering Research Center*, University of California Berkeley, CA.

Kawashima, K., Takahashi, Y., Ge, H., Wu, Z., Zhang, J. (2009). Damage of Bridges in 2008 Wenchuan, China Earthquake. *Journal of Earthquake Engineering*, **Vol.13**, 956-998.

Mazzoni, S., McKenna, F., Scott, M. H., and Fenves, G. L. (2006). OpenSees Command Language Manual.

Rodriguez, O., (2012) Seismic Demand Evaluation for a Three-span Curved Bridge Crossing Fault-Rupture Zones, *M.S. Thesis*, California Polytechnic State University.

Shantz, T., and Chiou, B. (2011). Creation of Record Set for Use in Fault Crossing Study. Division of Research and Innovation. California Department of Transportation.